Holzforschung, Vol. 61, pp. 182–189, 2007 • Copyright © by Walter de Gruyter • Berlin • New York. DOI 10.1515/HF.2007.032

Simple estimation of critical stress intensity factors of wood by tests with double cantilever beam and three-point end-notched flexure

Hiroshi Yoshihara*

Faculty of Science and Engineering, Shimane University, Matsue, Shimane, Japan

*Corresponding author.
Faculty of Science and Engineering, Shimane University, Nishikawazu-cho 1060, Matsue, Shimane 690-8504, Japan
E-mail: yosihara@riko.shimane-u.ac.jp

Abstract

Simple equations are proposed for calculation of critical stress intensity factors by tests using double cantilever beam (DCB) and three-point end-notched flexure (3ENF). The calculation modes are named here as modes I and II and are based on the beam theory and 95 previously published data on the elasticity properties of woods. The validity of the data was examined on specimens of western hemlock wood with various crack lengths. The influence of the elastic properties is more significant on the stress intensity factor calculated in mode I than that calculated in mode II. Further work is needed, particularly for measuring the mode I stress intensity factor. However, it is obvious from the experiments with western hemlock that the critical stress intensity factors can be determined by the equations proposed here.

Keywords: critical stress intensity factor; DCB test; 3ENF test; mode I; mode II; wood.

Introduction

Recently, it has become common practice to investigate cracks based on the energy release rate G rather than stress intensity factor K, because the former is mathematically well defined and experimentally measurable (Adams et al. 2003). The calculations of the mode I and mode II fracture characteristics rely on tests with double cantilever beam (DCB) and end-notched flexure (ENF) approaches, respectively. Here, the fracture toughness G_{Ic} and G_{IIc} can be defined mathematically according to the beam theory. Fracture toughness measurement with the DCB and ENF tests has been increasingly applied (Morel et al. 2002, 2003, 2005; Jensen 2005; Yoshihara 2005, 2006a,b; de Moura et al. 2006; Silva et al. 2006; Yoshihara and Kawamura 2006). Nevertheless, both techniques have a drawback: the load-deflection relation, which is mandatory for determining the fracture toughness, often deviates from the elementary beam theory because the deformation around the crack tip cannot be predicted.

There are three ways to correct the deformation around the crack tip. 1) A factor for correcting the crack length to the solution (Williams 1989; Chatterjee 1991; Wang and Williams 1992; Corleto and Hogan 1995; Williams and Hadavinia 2002) can be introduced. The elastic constant of the beam is needed for this approach, and it must be measured in separate tests. 2) The equivalent crack length corrected by the loading-line compliance can be used instead of the actual crack length (Blackman et al. 2005; de Moura et al. 2006; Silva et al. 2006). Separate tests are not necessary for measuring this parameter. 3) The strain at a certain point of the specimen can be measured (Yoshihara 2005, 2006a,b; Yoshihara and Kawamura 2006). The deflection and strain should be measured simultaneously, along with the applied load.

Besides the tests discussed above, there are more possibilities for measuring fracture properties. Compact tension (CT), single-edge notched tension (SENT), double-edge notched tension (DENT), and single-edge notched bending (SENB) tests have been described for measuring the fracture properties in mode I (Schniewind and Pozniak 1971; Mall et al. 1983; Triboulot et al. 1984; Kretschmann and Green 1996; King et al. 1999), whereas compact shear (CS), and double-edge notched shear (DENS) tests have been developed for measuring the fracture properties in mode II (Mall et al. 1983; Cramer and Pugel 1987; Prokopski 1995; Stanzl-Tschegg et al. 1996; Xu et al. 1996). In these methods, the critical stress intensity factor K_c is usually calculated by approximating equations instead of deriving the fracture toughness G_c. These equations often depend on the critical load for crack propagation and specimen configuration alone, and they do not contain any load-deflection relation or elastic constants of the material.

In terms of simplicity, measurement of K_c using an approximating equation is more advantageous than that of G_c. This idea may be applicable to DCB and ENF tests, but it would be desirable to determine the critical stress intensity factors K_{Ic} and K_{IIc} in the course of the tests. Nevertheless, publications are rare in this field (Barrett and Foschi 1977).

In the present work, DCB and three-point ENF (3ENF) tests were conducted and the critical stress intensity factors were analyzed by simple approximating equations derived from the beam theory. The validity of the equations was examined by comparing the results with experimental data.

Theories

Figure 1 shows diagrams of the DCB and 3ENF tests, for which specimens were prepared by cutting a crack along the neutral axis of a rectangular bar. As shown in Figure 1a, the load was applied to the upper and lower cantilever portion of the specimen in opposite directions to each other in the DCB test, whereas in the 3ENF test the load was applied to the midspan (Figure 1b). When neglecting the transverse shear deflection and considering the deformation around the crack tip, the deflection

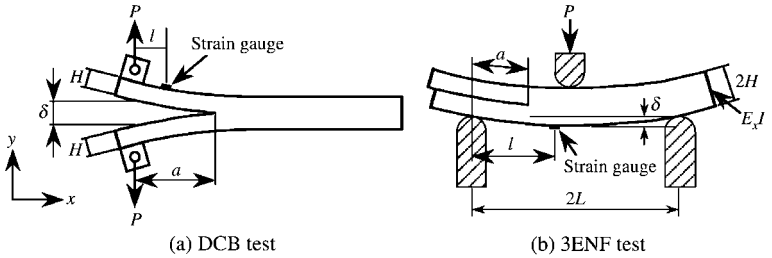

Figure 1 Schematic diagram of DCB and 3ENF tests.

at the loading point δ is derived by the modified beam theory, as follows (Adams et al. 2003):
DCB:

$$\delta = \frac{8P(a+\chi_I H)^3}{E_x B H^3} \tag{1}$$

3ENF:

$$\delta = \frac{P[2L^3+3(a+\chi_{II}H)^3]}{8E_x B H^3}, \tag{2}$$

where P is the applied load, a is the crack length, E_x is Young's modulus in the longitudinal axis, B is the width of the specimen, $2H$ is the depth of the specimen, $2L$ is the span length in the 3ENF test, and χ_I and χ_{II} are factors for correcting the crack length in the DCB and 3ENF tests, respectively. These factors are ignored in the elementary beam theory.

There are various theoretical models for deriving these correction factors χ_I and χ_{II} (Williams 1989; Chatterjee 1991; Wang and Williams 1992; Corleto and Hogan 1995; Williams and Hadavinia 2002). The question as to which model is most applicable cannot be answered yet. According to the Williams and Hadavinia model, these factors are given by the elastic constants of the beam (Williams and Hadavinia 2002; Adams et al. 2003) as:

$$\chi_I = \sqrt{0.24\sqrt{\frac{E_x}{E_y}}+0.1\left(\frac{E_x}{G_{xy}}-2\nu_{xy}\right)} \tag{3}$$

$$\chi_{II} = 0.42\sqrt{0.24\sqrt{\frac{E_x}{E_y}}+0.1\left(\frac{E_x}{G_{xy}}-2\nu_{xy}\right)}, \tag{4}$$

where E_y is Young's modulus in the depth direction, and G_{xy} and ν_{xy} are the shear modulus and Poisson's ratio in the length-depth plane, respectively. The loading-line compliance C_L is derived by δ/P, so:

DCB:

$$C_L = \frac{8(a+\chi_I H)^3}{E_x B H^3} \tag{5}$$

3ENF:

$$C_L = \frac{2L^3+3(a+\chi_{II}H)^3}{8E_x B H^3}. \tag{6}$$

The energy release rates in modes I and II, G_I and G_{II}, respectively, are given as:

$$G_I = \frac{P^2}{2B}\cdot\frac{\partial C_L}{\partial a} = \frac{12P^2(a+\chi_I H)^2}{E_x B^2 H^3} \tag{7}$$

$$G_{II} = \frac{9P^2(a+\chi_{II}H)^2}{16E_x B^2 H^3}. \tag{8}$$

It is time-consuming to determine the energy release rates by Eqs. (7) and (8) because the elastic constants E_x, E_y, G_{xy}, and ν_{xy} that include χ_I and χ_{II} should be measured by separate tests independently of the fracture test. Nevertheless, this obstacle can be overcome when the longitudinal strain is measured simultaneously at a certain point of the beam, together with the loading point deflection. When the longitudinal strain on the bottom surface of a specimen ε_x is measured at a point located at $x=l$ ($0<l<a$ in the DCB test and $a<l<2L$ in the 3ENF test) – as shown in Figure 1 – the load-strain compliance C_S, which is defined as ε_x/P, is derived by the beam theory independently of the crack length as follows:

DCB:

$$C_S = \frac{6l}{E_x B H^2} \tag{9}$$

3ENF:

$$C_S = \frac{3l}{4E_x B H^2}. \tag{10}$$

From Eqs. (5), (6), (9), and (10), $a+\chi_I H$ and $a+\chi_{II}H$ are written as follows:

$$a+\chi_I H = \left(\frac{3Hl}{4}\cdot\frac{C_L}{C_S}\right)^{\frac{1}{3}} \tag{11}$$

$$a+\chi_{II}H = \left(2Hl\cdot\frac{C_L}{C_S}-\frac{2}{3}L^3\right)^{\frac{1}{3}}. \tag{12}$$

By substituting Eqs. (9) and (11) into Eq. (7), E_x and χ_I are eliminated and G_I is derived as follows:

$$G_I = \frac{3P^2C_L}{2B}\left(\frac{3Hl}{4}\cdot\frac{C_L}{C_S}\right)^{-\frac{1}{3}}. \tag{13}$$

Similarly, G_{II} is derived by substituting Eqs. (10) and (12) into Eq. (8) as follows:

$$G_{II} = \frac{3P^2C_S}{4BLH}\left(2Hl\cdot\frac{C_L}{C_S}-\frac{2}{3}L^3\right)^{\frac{2}{3}}. \tag{14}$$

Equations (13) and (14) signify that the energy release rates G_I and G_{II} can be independently obtained directly by the DCB and 3ENF fracture tests, respectively, while correcting the influences of transverse shear force and crack tip deformation. The author previously called this approach the "compliance combination method", and verified that the fracture toughness can be obtained appropriately by modes I and II (Yoshihara 2005, 2006a,b; Yoshihara and Kawamura 2006).

The energy release rates G_I and G_{II} can be transformed into the stress intensity factors K_I and K_{II}, respectively, when using the following relations (Sih et al. 1965):

$$K_I = \sqrt{\frac{E_x G_I}{\alpha_I}} \tag{15}$$

$$K_{II} = \sqrt{\frac{E_x G_{II}}{\alpha_{II}}}, \tag{16}$$

where

$$\alpha_I = \frac{1}{\sqrt{2}} \sqrt{\frac{E_x}{E_y}} \sqrt{\sqrt{\frac{E_x}{E_y}} + \frac{1}{2}\left(\frac{E_x}{G_{xy}} - 2\nu_{xy}\right)} \tag{17}$$

$$\alpha_{II} = \frac{1}{\sqrt{2}} \sqrt{\sqrt{\frac{E_x}{E_y}} + \frac{1}{2}\left(\frac{E_x}{G_{xy}} - 2\nu_{xy}\right)}. \tag{18}$$

By substituting Eqs. (7) and (8) into Eqs. (15) and (16), respectively, the stress intensity factors are derived as follows:

DCB:

$$K_I = \frac{P}{B\sqrt{H}}\left(p_I \cdot \frac{a}{H} + q_I\right) \tag{19}$$

3ENF:

$$K_{II} = \frac{P}{B\sqrt{2H}}\left(p_{II} \cdot \frac{a}{2H} + q_{II}\right), \tag{20}$$

where

$$\begin{cases} p_I = \sqrt{\dfrac{12}{\alpha_I}} \\ q_I = \chi_I \sqrt{\dfrac{12}{\alpha_I}} \end{cases} \tag{21}$$

$$\begin{cases} p_{II} = 3\sqrt{\dfrac{1}{2\alpha_{II}}} \\ q_{II} = \dfrac{3\chi_{II}}{2}\sqrt{\dfrac{1}{2\alpha_{II}}} \end{cases} \tag{22}$$

As represented by Eqs. (17), (18), (21), and (22), the parameters p_I, q_I, p_{II}, and q_{II} include the elastic constants E_x, E_y, G_{xy}, and ν_{xy}, so K_I and K_{II} are dependent on the elastic properties of the test material. When these parameters are approximated using constants, K_I and K_{II} can be obtained simply by the specimen configuration, crack length, and applied load.

For example, Murphy (1979, 1988) proposed a center slit flexure test for measuring the mode II stress intensity factor, and derived p_{II} and q_{II} as 1.4 and 0.36, respectively, by averaging the values of several wood species. From 95 data on the elastic constants for the longitudinal-tangential and longitudinal-radial planes of 25 hardwood and 10 softwood species collected by Hearmon (1948), Kollmann and Côte (1968), and the Forestry and Forest Products Research Institute Japan (2004), the values of E_x/E_y and $E_x/G_{xy} - 2\nu_{xy}$ were found to be in the range of 8–28 for hardwoods and 11–23 for softwoods.

Material and methods

Specimens

Western hemlock (*Tsuga heterophylla* Sarg.) lumber, with a density of 0.48 ± 0.01 g cm^{-3} at 12% moisture content (MC), was tested. As shown in Figure 2, the annual rings were flat enough to ignore their curvature. This lumber had no defects (knots or grain distortions) so that the specimens cut from it could be regarded as "small and clear". The lumber was stored before the test for approximately 1 year in a room at 20°C and 65% relative humidity. The equilibrium MC condition was approximately 12%.

Compression tests

Young's moduli E_x and E_y, shear modulus G_{xy}, and Poisson's ratio ν_{xy} are required for transforming the energy release rates obtained by the beam theory and compliance combination methods. With this aim, the stress intensity factor was obtained using Eqs. (15) and (16). These elastic constants were determined by compression tests.

A short-column specimen with the dimensions of 40 mm×20 mm×20 mm was prepared from the lumber described above. When measuring E_x and ν_{xy}, the long axis of the specimen was coincident with the longitudinal direction of wood, whereas when measuring E_y, the long axis of the specimen was aligned with the tangential direction. When measuring G_{xy}, the long axis was inclined at 45° to the grain. Strain gauges

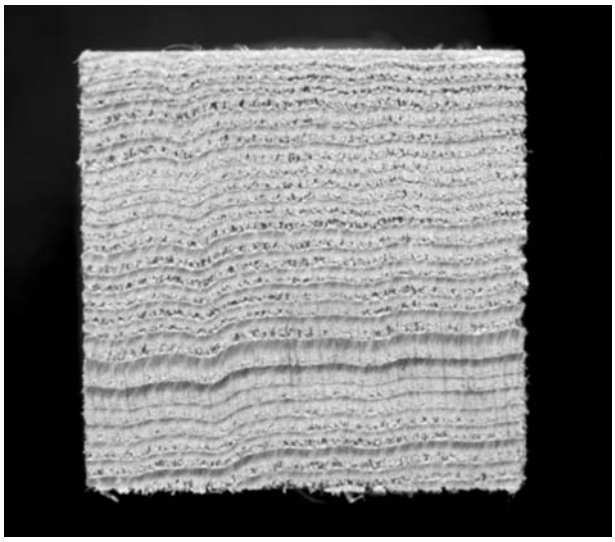

Figure 2 Image of a cross-section of the material used in this experiment.

were bonded at the centers of longitudinal-tangential planes, and compression load was applied along the long axis of the specimen at a crosshead speed of 1 mm min^{-1}. Young's moduli E_x and E_y were obtained from the stress-strain relation in the loading direction. Poisson's ratio ν_{xy} was obtained by the relation between the longitudinal and tangential strains by applying the compression load in the longitudinal direction.

For the 45° inclined specimen, Young's modulus in the loading direction E_{45} was obtained from the stress-strain relation. The strain in the direction perpendicular to the loading axis was simultaneously measured, and Poisson's ratio ν_{45} was obtained, as well as Young's modulus E_{45}. The shear modulus G_{xy} was determined from the following equation:

$$G_{xy} = \frac{E_{45}}{2(1+\nu_{45})}. \quad (23)$$

The averages of E_x, E_y, G_{xy}, and ν_{xy} were substituted into Eqs. (3), (4), (17), and (18), and the fracture toughness G_{Ic} and G_{IIc} (obtained by the beam theory and by the compliance combination methods) were transformed into the critical stress intensity factors K_{Ic} and K_{IIc}, respectively.

DCB tests

The dimensions of the specimens were 15 mm×15 mm×315 mm (R×T×L). A crack was produced along the longitudinal direction in the longitudinal-tangential plane, which is the so-called TL system. The crack was first cut with a band saw (thickness 1 mm), and then extended 1 mm ahead of the crack tip using a razor blade.

Loading blocks of western hemlock with dimensions of 30 mm in length, 30 mm in height, and 15 mm in thickness were bonded by epoxy resin on the upper and lower cantilever portions opposite each other (Figure 1). Crack length, which was defined as the distance from the line of load application to the crack tip, varied from 60 to 160 mm in intervals of 20 mm. Load was applied to the specimen by pins through universal joints at a crosshead speed of 5 mm min^{-1} until the load markedly decreased. The total testing time was approximately 10 min (five repetitions).

The loading-line displacement δ was measured by the crosshead travel, since it was confirmed that the machine compliance was small enough to be ignored (Yoshihara and Kawamura 2006), whereas the longitudinal strain ε_x was measured using a strain gauge (gauge length 2 mm; FLA-2-11, Tokyo Sokki Co., Tokyo) bonded at the midpoint between the loading line and crack tip on the top cantilever portion ($l = a/2$), in a location similar to that in previous work (Yoshihara and Kawamura 2006). The loading-line compliance C_L and the load-longitudinal strain compliance C_S were obtained from the linear portions of P-δ and P-ε_x relations, respectively.

As shown in Figure 3, the critical load for crack propagation P_c was defined as the load at the intersection point between the load-loading line displacement curve and straight line with a 5% increase in compliance (Yoshihara 2005, 2006a; Yoshihara and Kawamura 2006). By substituting P_c, C_L, and C_S into Eq. (13), the mode I fracture toughness G_{Ic} was obtained. Then the value of G_{Ic} was transformed into the critical stress intensity factor K_{Ic} using Eq. (15).

3ENF tests

Similar to the DCB tests, all of the specimens were cut from the lumber described above. The initial dimensions were 15 mm×15 mm×450 mm (R×T×L). The crack was cut in the same manner as for the DCB tests, and the crack length varied from 60 to 160 mm in intervals of 20 mm. Two sheets of 0.5-mm-thick Teflon film were inserted between the crack surfaces to reduce the friction between the upper and lower cantilever beams.

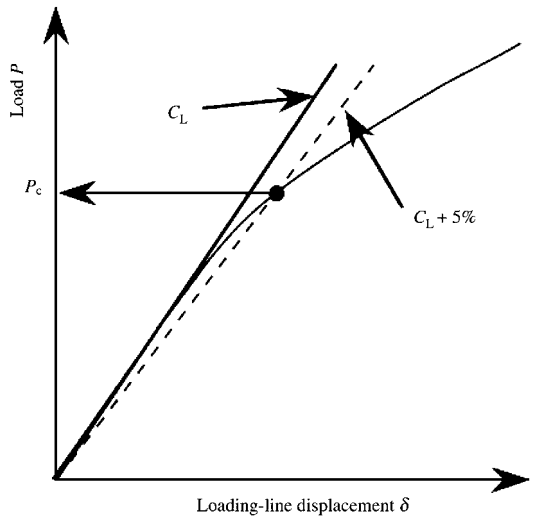

Figure 3 Definition of critical load P_c.

These specimens were supported by 400-mm spans, and a load was applied to the midspan at a crosshead speed of 2 mm min^{-1} until significant non-linearity in the load-loading line displacement relation was induced. The total testing time was approximately 10 min. Five specimens were used for one testing condition. To avoid the influence of indentation of the loading nose, the loading-line deflection δ was measured by an LVDT set below the specimen, whereas the longitudinal strain ε_x was measured using a strain gauge (gauge length 2 mm; FLA-2-11) bonded to the bottom surface of the midspan ($l = L$). The loading-line compliance C_L and load-longitudinal strain compliance C_S were obtained from the linear portions of P-δ and P-ε_x relations, respectively.

According to the elementary beam theory, a fracture propagates unstably when the crack length is smaller than 0.7 times the half-span length (Carlsson et al. 1986). In the 3ENF tests conducted here, however, the crack propagated stably in every specimen because of the large value of additional crack length $\chi_{II}H$ (Yoshihara 2005). Hence, the critical load for crack propagation was determined as the load at the intersection point between the load-loading line displacement and a straight line with a 5% increase in compliance, similar to the DCB test. By substituting P_c, C_L, and C_S into Eq. (14), the mode II fracture toughness G_{IIc} was obtained. Then the value of G_{IIc} was transformed into the critical stress intensity factor K_{IIc} using Eq. (16).

Analysis methods

The critical stress intensity factors were analyzed by the following six methods: modified beam theory, compliance combination, and linear approximations A, B, C, and D. The details are described below.

In applying the modified beam theory, the fracture toughness G_{Ic} was calculated by substituting Young's modulus E_x, critical load P_c, initial crack length a_0, and correction factor χ_I into Eq. (7), whereas G_{IIc} was calculated by substituting E_x, P_c, a_0, and χ_{II} into Eq. (8). Then the values of G_{Ic} and G_{IIc} were transformed into K_{Ic} and K_{IIc}, respectively, by substituting these values and E_x, E_y, G_{xy}, and ν_{xy} into Eqs. (15) and (16), respectively.

In the compliance combination method, G_{Ic} and G_{IIc} were obtained by substituting P_c, C_L, and C_S into Eqs. (13) and (14), respectively, then transformed into the critical stress intensity factors in the same manner as for the modified beam theory method.

In the linear approximation methods, the values of K_{Ic} and K_{IIc} were obtained by substituting P_c into Eqs. (19) and (20), respectively, but the values of the parameters were different in methods A–D. In methods A and B, the parameters were derived from the data for compression tests on western hemlock and 95 data from the literature (Hearmon 1948; Kollmann and Côte 1968; Forestry and Forest Products Research Institute Japan 2004), respectively. When comparing χ_I for western hemlock obtained from Eqs. (3) and (11), however, χ_I obtained from Eq. (11) was 2.45±0.66, approximately 1.5-fold greater than the value obtained from Eq. (3), which was 1.62. Similarly, χ_{II} obtained from Eq. (12) was 3.67±1.12, approximately five-fold greater than the value obtained from Eq. (4), which was 0.68. Several researchers have suggested that Eqs. (3) and (4) are no longer valid when a fracture process zone, which is the region where the material progressively softens, develops at the crack tip (de Moura et al. 2006; Silva et al. 2006). Considering the exaggerated values of χ_I and χ_{II}, the values of q_I and q_{II} were thus corrected in methods C and D. In method C, the elastic constants obtained from compression tests on western hemlock were used, but the values of q_I and q_{II} were corrected as follows:

$$q_I = 1.5\chi_I\sqrt{\frac{12}{\alpha_I}} \tag{24}$$

$$q_{II} = 7.5\chi_{II}\sqrt{\frac{1}{2\alpha_{II}}}. \tag{25}$$

In these equations, χ_I and χ_{II} were derived by Eqs. (3) and (4), respectively. In method D, the elastic constants were from 95 data obtained from the literature, and the values of q_I and q_{II} were derived by Eqs. (24) and (25), respectively.

Results and discussion

Figure 4 shows the dependence of the parameters p_I, q_I, p_{II}, and q_{II} on the values of E_x/E_y and $E_x/G_{xy}-2\nu_{xy}$. The influence of variation in the elastic constants is rather significant on the values of p_I and q_I. This indicates that K_I might not be properly obtained when some constant values are derived for p_I and q_I. When the value of E_x/E_y is restricted to the range from 11 to 24, however, variations in p_I and q_I are approximately within 20%. In contrast, the influence of variation in the elastic constants is rather small on the values of p_{II} and q_{II}, so that determination of K_{II} by this method is promising. K_{II} is probably more correct than K_I in view of the wide range of possible elastic properties.

Table 1 Elastic properties used for the transformation of energy release rates G_I and G_{II} into stress intensity factors K_I and K_{II}, respectively.

E_x (GPa)	E_y (GPa)	G_{xy} (GPa)	ν_{xy}
14.9±0.4	0.73±0.10	0.90±0.11	0.51±0.02

Results are mean±SD.

Table 1 lists Young's moduli in the longitudinal and tangential directions, E_x and E_y, respectively, and the shear modulus and Poisson's ratio on the longitudinal-tangential plane, G_{xy} and ν_{xy}, respectively, for western hemlock obtained from compression tests. From the averages of these elastic constants, the values of E_x/E_y and $E_x/G_{xy}-2\nu_{xy}$ used in linear approximation methods A and C were derived as 20.4 and 15.5, respectively. By substituting these values into Eqs. (17), (18), (21), (22), (24), and (25), the parameters p_I, q_I, p_{II}, and q_{II} were obtained as listed in Table 2. The values of p_I, q_I, p_{II}, and q_{II} (Table 2) were obtained from a similar procedure applied to 95 data taken from the literature.

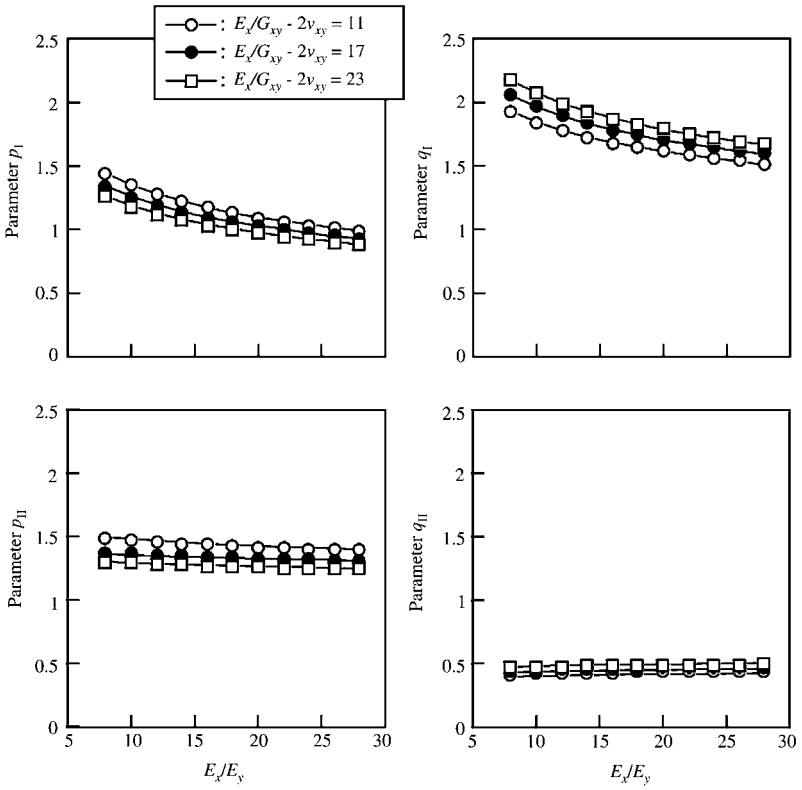

Figure 4 Dependence of the parameters p_I, q_I, p_{II}, and q_{II} on the elastic properties E_x/E_y and $E_x/G_{xy}-2\nu_{xy}$.

Table 2 Parameters p_I, q_I, p_{II}, and q_{II} for deriving stress intensity factors in the linear approximation methods.

Method	Mode I		Mode II	
	p_I	q_I	p_{II}	q_{II}
A	1.04	1.68	1.35	0.46
B	1.13±0.22	1.78±0.13	1.36±0.10	0.46±0.03
C	1.04	2.52	1.35	2.30
D	1.13±0.22	2.63±0.20	1.36±0.10	2.25±0.18

The parameters in methods A and C were obtained from compression test data for western hemlock, whereas those in methods B and D were given by the 95 data reported by Hearmon (1948), Kollmann and Côte (1968), and the Forestry and Forest Products Research Institute Japan (2004). Data for B and D are mean±SD.

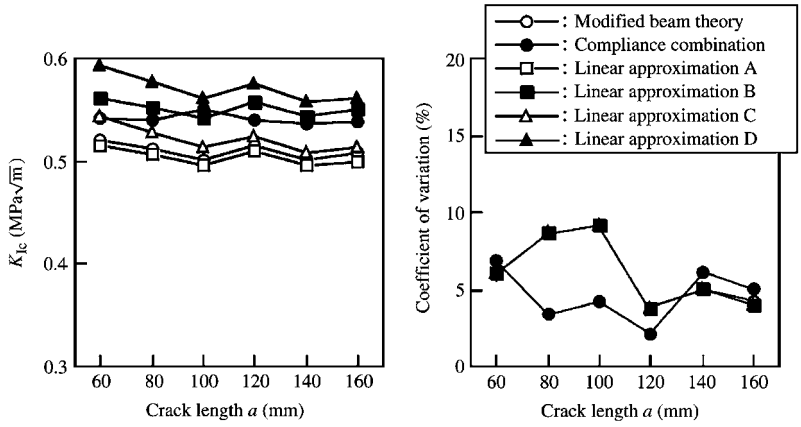

Figure 5 Comparison of the relations between the mode I critical stress intensity factor K_{Ic} and crack length a obtained by each analytical method.

Figure 5 shows comparisons of K_{Ic} corresponding to the crack length a obtained by each analytical method. The influence of crack length is not significant on K_{Ic}, and statistical analyses reveal that there are no differences between the values of K_{Ic} obtained by the six methods at the significance level of 0.01. As mentioned above, variations in p_I and q_I are approximately within 20% for E_x/E_y in the range from 11 to 24. Since the value of E_x/E_y for western hemlock used here was 20.4, K_{Ic} could be obtained appropriately.

In methods A and C, the parameters obtained for a specific species are needed, so there is a concern that K_{Ic} for another species cannot be measured by these methods. Among the 95 data analyzed, 53 data satisfy E_x/E_y in the range 11–24, so it is feasible to obtain K_{Ic} for rather various species by methods B and D. As described in previous work, the mode I fracture toughness can be obtained by the compliance combination method more appropriately than deriving the correction factor χ_I from the elastic constants (Yoshihara and Kawamura 2006). When comparing methods B and D, method D – in which the compliance combination method is used to determine the value of q_I – is more appropriate than method B, in which q_I is obtained using χ_I consisting of

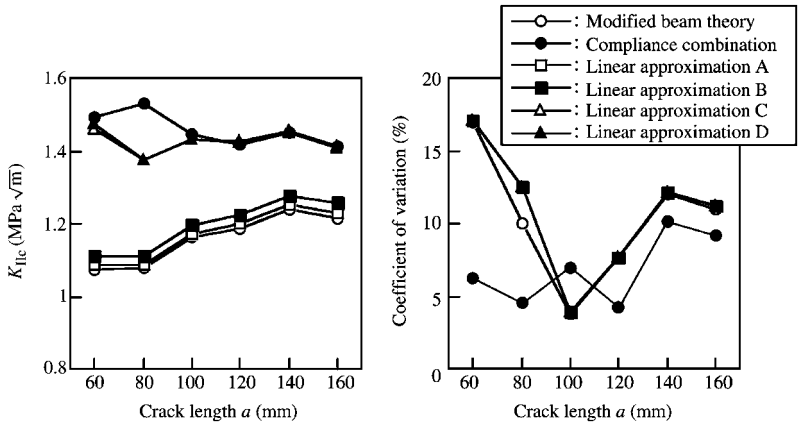

Figure 6 Comparison of the relations between the mode II critical stress intensity factor K_{IIc} and crack length a obtained by each analytical method.

the elastic constants. Therefore, the following relation is proposed for obtaining the mode I stress intensity factor from DCB tests:

$$K_{\mathrm{I}} = \frac{P}{B\sqrt{H}}\left(1.13\frac{a}{H} + 2.63\right). \quad (26)$$

Figure 6 shows a comparison of the mode II critical stress intensity factor K_{IIc} corresponding to crack length a obtained by each analytical method. The influence of crack length is not significant for values of K_{IIc} obtained by the compliance combination and by linear approximation methods C and D. Nevertheless, statistical analyses reveal that K_{IIc} values obtained by the modified beam theory and by linear approximation methods A and B were smaller than those obtained by the other methods at significance level 0.01 when the crack length was smaller than 120 mm. Murphy (1988) conducted an asymmetric four-point bending test on a specimen with a center slit to measure K_{IIc}, and derived values of 1.4 for p_{II} and 0.36 for q_{II}. The value of K_{IIc} for clear Douglas fir tended to decrease when the crack length was decreased. This tendency is similar to the K_{IIc}-a relations obtained by the modified beam theory and linear approximations A and B. This can be explained by the small value of q_{II} used in these methods. In addition, the influence of variations in the elastic constants is rather small on the data for p_{II} and q_{II}. Accordingly, linear approximation D, which is based on data for various species, is recommended for deriving the K_{IIc}-a relation, and the following relation is proposed for obtaining the mode II stress intensity factor from 3ENF tests:

$$K_{\mathrm{II}} = \frac{P}{B\sqrt{2H}}\left(1.36\frac{a}{2H} + 2.25\right). \quad (27)$$

As mentioned above, there is a concern that Eq. (26) is not effective when measuring the mode I stress intensity factor of a material if E_x/E_y is outside the range 11–24. On the other hand, Eq. (27) is applicable for measuring the mode II stress intensity factor. To verify the broad validity range for the proposed method, further research is needed on DCB and 3ENF tests and various wood species should be included in the test program.

Conclusions

To obtain critical stress intensity factors according to modes I and II by DCB and 3ENF tests, equations are proposed based on the beam theory. Data on elastic properties previously published were used to validate the data obtained from western hemlock with various crack lengths.

The influence of elastic properties is more significant for measuring the mode I stress intensity factor than that of mode II. The mode I stress intensity factor needs more attention in the future. As for the specimens of western hemlock examined here, however, both stress intensity factors could be properly obtained, and it appears that the critical stress intensity factors can be determined by the equations proposed here.

Acknowledgements

The author would like to thank Prof. Tohru Uehara of Shimane University for his help in conducting the experiment.

References

Adams, D.F., Carlsson, L.F., Pipes, R.B. Experimental Characterization of Advanced Composite Materials, 3rd ed. CRC Press, Boca Raton, 2003.

Barrett, J.D., Foschi, R.O. (1977) Mode II stress-intensity factors for cracked wood beams. Eng. Fract. Mech. 9:371–378.

Blackman, B.R.K., Kinloch, A.J., Paraschi, M. (2005) The determination of the mode II adhesive fracture resistance, G_{IIc}, of structural adhesive joints: an effective crack length approach. Eng. Fract. Mech. 72:877–897.

Carlsson, L.A., Gillespie, J.W. Jr., Pipes, R.B. (1986) On the analysis and design of the end notched flexure (ENF) specimen for mode II testing. J. Compos. Mater. 20:594–604.

Chatterjee, S.N. (1991) Analysis of test specimens for interlaminar mode II fracture toughness. J. Compos. Mater. 25:470–493.

Corleto, C.R., Hogan, H.A. (1995) Energy release rates for the ENF specimen using a beam on an elastic foundation. J. Compos. Mater. 29:1420–1436.

Cramer, S.M., Pugel, A.D. (1987) Compact shear specimen for wood mode II fracture investigations. Int. J. Fract. 35:163–174.

de Moura, M.F.S.F., Silva, M.A.L., de Morais, A.B., Morais, J.J.L. (2006) Equivalent crack based mode II fracture characterization of wood. Eng. Fract. Mech. 73:978–993.

Forestry and Forest Products Research Institute Japan. Handbook of Wood Industry, 4th ed. Maruzen, Tokyo, 2004.

Hearmon, R.F.S. Elasticity of Wood and Plywood. HM Stationary Office, London, 1948.

Jensen, L.J. (2005) Quasi-non-linear fracture mechanics analysis of the double cantilever beam specimen. J. Wood Sci. 51: 566–571.

King, M.J., Sutherland, I.J., Le-Ngoc, L. (1999) Fracture toughness of wet and dry *Pinus radiata*. Holz Roh Werkst. 57:235–240.

Kollmann, F.F.P., Côte, W.A. Principles of Wood Science and Technology I. Springer-Verlag, Berlin, 1968.

Kretschmann, D.E., Green, D.W. (1996) Modeling moisture content-mechanical property relationships for clear southern pine. Wood Fiber Sci. 28:320–337.

Mall, S., Murphy, J.F., Shottafer, J.E. (1983) Criterion for mixed mode fracture in wood. J. Eng. Mech. 109:680–690.

Morel, S., Bouchaud, E., Schmittbuhl, J., Valentin, G. (2002) *R*-curve behavior and roughness development of fracture surfaces. Int. J. Fract. 114:307–325.

Morel, S., Bouchaud, E., Schmittbuhl, J. (2003) Influence of the specimen geometry on *R*-curve behavior and roughening of fracture surfaces. Int. J. Fract. 121:23–42.

Morel, S., Dourado, N., Valentin, G., Morais, J. (2005) Wood: a quasibrittle material *R*-curve behavior and peak load evaluation. Int. J. Fract. 131:385–400.

Murphy, J.F. (1979) Strength of wood beams with end splits. Report 347. USDA FPL, Madison, WI.

Murphy, J.F. (1988) Mode II wood test specimen: beam with center slit. J. Test. Eval. 4:364–368.

Prokopski, G. (1995) Investigation of wood fracture toughness using mode II fracture (shearing). J. Mater. Sci. 30:4745–4750.

Schniewind, A.P., Pozniak, R.A. (1971) On the fracture toughness of Douglas-fir wood. Eng. Fract. Mech. 2:223–233.

Sih, G.C., Paris, P.C., Irwin, G.R. (1965) On cracks in rectilinearly anisotropic bodies. Int. J. Fract. Mech. 1:189–203.

Silva, M.A.L., de Moura, M.F.S.F., Morais, J.J.L. (2006) Numerical analysis of the ENF test for mode II wood fracture. Composites A 37:1334–1344.

Stanzl-Tschegg, S.E., Tan, D.M., Tschegg, E.K. (1996) Mode II fracture tests on spruce wood. Mokuzai Gakkaishi 42:642–650.

Triboulot, P., Jodin, P., Pluvinage, G. (1984) Validity of fracture mechanics concepts applied to wood by finite element calculation. Wood Sci. Technol. 18:51–58.

Wang, Y., Williams, J.G. (1992) Corrections for mode II fracture toughness specimens of composites materials. Compos. Sci. Technol. 43:251–256.

Williams, J.G. (1989) The fracture mechanics of delamination tests. J. Strain Anal. 24:207–214.

Williams, J.G., Hadavinia, H. (2002) Analytical solutions for cohesive zone models. J. Mech. Phys. Solids 50:809–825.

Xu, S., Reinhardt, H.W., Gappoev, M. (1996) Mode II fracture testing method for highly orthotropic materials like wood. Int. J. Fract. 75:185–214.

Yoshihara, H. (2005) Mode II initiation fracture toughness analysis for wood obtained by 3-ENF test. Compos. Sci. Technol. 65:2198–2207.

Yoshihara, H. (2006a) Influence of crack length on the measurement of mode II initiation fracture toughness of wood by three-point bend end-notched flexure (3ENF) test. Trans. Jpn. Soc. Mech. Eng. A 72:133–139.

Yoshihara, H. (2006b) Examination of the 4-ENF test for measuring the mode III *R*-curve of wood. Eng. Fract. Mech. 73: 42–63.

Yoshihara, H., Kawamura, T. (2006) Mode I fracture toughness estimation of wood by DCB test. Composites A 37:2105–2113.

Received July 20, 2006. Accepted December 19, 2006.